

# Incipient Motion of Solid Particles on the Surface of a Submerged Rotating Disk

Nobuyuki Tamai , Professor  
Takashi Asaeda , Assoc. Professor  
Shyam K. Manandhar , Grad. Student  
Chaisak Sripadungtham , Grad. Student  
Yusuke Hirose , Research Assoc.  
University of Tokyo

## 1. Introduction

Several studies have been carried out on the motion of sediment particles on horizontal bed, transverse slope and longitudinal slope(3,6,7). Several criteria have been proposed for the critical tractive force on the non-cohesive sediment. However, in these studies, the particle is subjected to only the drag and the lift forces due to the flow field, and the gravitational flow. The present study is undertaken to analyze the critical tractive force equivalent on the particle which is in addition subjected to an external body force. A case of the incipient motion of the particle on the surface of a rotating disk, where the particle is subjected to the centrifugal force is studied. The steady motion of an incompressible viscous fluid, due to rotating disk is a case of fully three-dimensional flow. The case of an infinite rotating disk, as pointed out by Karman, constitutes a simple solution of Navier-Stokes equations. In Karman's problem, the fluid region is semi-infinite and the flow far from the disk is assumed to be wholly normal to the disk, and induced by the rotation of the disk. This problem has been solved by analytical-numerical method by Cochran(2) and later improved upon by Benton(1), for the case of laminar flow. For the turbulent motion of the flow due to rotation of the disk, studies have been reported by Karman, and Goldstein(5). In the present study, as a first step, for the laminar case, an expression for critical tractive force equivalent has been obtained, taking into consideration the drag and the lift forces on the particle due to the flow field generated by the motion of the disk. An experiment was carried out on the incipient motion of the particles, and the velocity profiles were measured. The analytical expression is checked with the experimental observation.

## 2. Analytical Consideration

The equilibrium equation for the incipient motion of a sand particle on the surface of the rotating disk can be written as

$$(W - T)^2 \tan^2 \phi = D_v^2 + (D_u + C)^2 \quad (1)$$

where  $W$  : submerged weight of the particle;  $T$  :  $L_u + L_v + L_p + D_u$ ;  $L_u$  and  $L_v$  : lift forces due to slip  $w$  shear effect caused by the velocity gradient in radial and circumferential direction respectively;  $L_p$  : lift force due to the pressure difference;  $D_u$  : Drag force due to axial velocity  $w$ ;  $D_v$  : drag force in circumferential direction;  $C$  : drag force in radial direction;  $C$  : centrifugal force;  $\phi$  : angle of friction of the particle. All the forces are assumed to be acting at the center of the particle. Introducing  $\epsilon$  as the ratio of the centrifugal force to the submerged weight of the particle, and

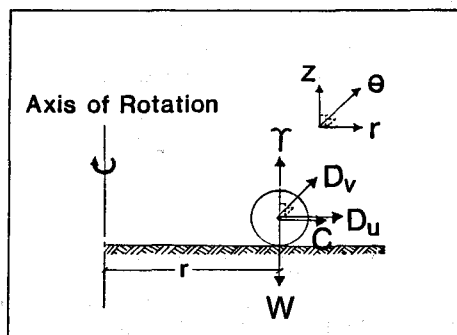


Fig.1 Forces in Equilibrium

non-dimensionalizing with division by the factor  $\rho \pi d^2 \omega^2 r^2 / 6$ , the non-dimensional critical tractive force equivalent defined by  $\tau_c = 1/\omega^0 = \omega^2 r^2 / \{(\sigma/\rho - 1)gd\}$ ;  $\omega$ : angular velocity of the disk,  $r$ : radius,  $\sigma$  and  $\rho$ : mass densities of particles and fluid respectively,  $g$ : acceleration due to gravity,  $d$ : diameter of particle; , can be expressed as

$$\tau_c = \frac{-(\tau_c \tan^2 \phi + \epsilon D_{u_0}) + \sqrt{(\epsilon^2 \tau_c^2 + 2\epsilon \tau_c D_{u_0} + D_{u_0}^2 + D_{v_0}^2) \tan^2 \phi - \epsilon^2 D_{v_0}^2}}{D_{u_0}^2 + D_{v_0}^2 - \tau_c \tan^2 \phi} \quad (2)$$

where various non-dimensional terms using the notation

$$\begin{aligned} u(r, z) &= r\omega F(\xi) & w(z) &= (\nu\omega)^{1/2} H(\xi) \\ v(r, z) &= r\omega G(\xi) & \xi &= z\sqrt{\omega/\nu} = R_d/2R_r^{1/2} \\ p(z) &= p\nu\omega P(\xi) \end{aligned} \quad (3)$$

are defined as

$$\begin{aligned} D_{u_0} &= 0.75 C_{D_u} F|F| & \epsilon &= \frac{\sigma}{\sigma - \rho} \frac{\omega^2 r}{g} \\ D_{v_0} &= 0.75 C_{D_v} (1-G)|1-G| & C_{D_u} &= C_d(R_d|F|) \\ D_{w_0} &= 0.75 C_{D_w} \frac{H|H|}{R_r} & C_{D_v} &= C_d(R_d|1-G|) \\ L_{u_0} &= 0.75 C_{L_u} F|F| \cdot |F'|/F' & C_{D_w} &= C_d \frac{(R_d|H|)}{R_r^{1/2}} \\ L_{v_0} &= 0.75 C_{L_v} (1-G)|1-G| \cdot |-G'|/(-G') & & \\ L_{p_0} &= 1.5 \frac{P-P}{R_r} \end{aligned} \quad (4)$$

where various coefficients are given by(4,8,9),

$$C_d(f) = \begin{cases} 24/f & 0.5 < f \\ 24/f + 3/\sqrt{f} + 0.34 & 0.5 \leq f \leq 10,000 \\ 0.4 & 10,000 < f \end{cases} \quad C_{L_u} = \frac{2K}{\pi F} \left( \frac{(dF/d\xi)}{R_r^{1/2}} \right)^{1/2} \quad (5)$$

$$C_{L_v} = \frac{2K}{\pi(1-G)} \left( \frac{(dG/d\xi)}{R_r^{1/2}} \right)^{1/2} \quad (6)$$

where  $K = 81.2$

with the Reynolds numbers defined as

$$R_d = \frac{\omega r d}{\nu} \quad R_r = \frac{\omega r^2}{\nu}$$

### 3. Relative magnitudes of various forces

The range of Reynolds number  $R(=\omega r \delta/\nu)$ , where  $\delta$ : boundary layer thickness  $\sim 0.5$ cm, encountered in the experiments performed is less than the critical Reynolds number for flat plate defined by  $R_{crit}$  ( $\sim 8890$ ) based the boundary layer thickness(10). Hence the flow could be assumed to be laminar. Solution of the Karman rotating disk

problem for laminar flow following Benton can be expressed as follows:

$$F = \frac{s^2}{2} \sum_{j=1}^n j b_j \lambda^j ; \quad F' = \frac{s^3}{2} \sum_{j=1}^n -j^2 b_j \lambda^j ; \quad H = s \left( \sum_{j=1}^n b_j \lambda^{j-1} \right) \quad (7)$$

$$G = s^2 \sum_{j=1}^n j a_j \lambda^j ; \quad G' = s^3 \sum_{j=1}^n -j a_j \lambda^j ; \quad P-P_0 = \frac{H^2}{2} + 2F$$

where

$$a_j = \frac{1}{j(j-1)} \sum_{k=1}^{j-1} (j-2k) a_k b_{j-k} ; \quad j = 2, 3, \dots, n \quad (8)$$

$$b_j = \frac{-1}{2j^2(j-1)} \sum_{k=1}^{j-1} (j-k)(2j-3k) b_k b_{j-k} + 4a_k a_{j-k} ; \quad j = 2, 3, \dots, n$$

with

$$s = .88447 ; \quad b_1 = 2.36449 ; \quad a_1 = 1.53678$$

Under the above velocity profiles, for the range of conditions encountered in the experimental observations, the relative magnitudes of various terms expressed as multiple of centrifugal force are as follows:

$\omega$	$r$	$R_r$	$R_d$	$D_u$	$D_v$	$D_w$	$L_p$	$L_u$	$L_v$
1.45	18	5501	30.6	4.87	7.48	.012	.003	17.2	34.0
3.04	10	3559	35.6	3.23	5.54	.014	.004	12.5	29.8
1.23	18	4666	51.8	2.53	4.87	.011	.003	11.1	31.0
2.57	10	3009	60.2	1.58	3.72	.012	.003	6.38	25.7

Based on above analysis, it was decided that the terms  $D_w$  and  $L_p$  could be neglected.

#### 4. Experimental Set-up

A metallic disk of diameter 40cm, surface coated with fine sand, was positioned on the threaded axle of diameter 2cm, passing through the center of the disk and resting on a bearing plate. A pulley attached to the axle as shown in Fig.2 was belt-driven by a motor, which could be adjusted for different speed. Spherical glass beads, of specific gravity 2.65, and diameters 1mm, and 2mm were used to observe the incipient motion. The angle of friction between the beads and the disk surface measured by tilting the similar surface with particles on it, was average out to be 45° for approximately 50% particle movement. The viscosity of the fluid used, 50% glycerine-water mixture, was measured with Ostwald type viscometer and found to be .0854 cm<sup>2</sup>/s. The specific gravity of the fluid measured with hydrometer was found to be 1.147. The fluid above the disk was kept to a depth of 10cm and was contained in a cylindrical vessel of diameter 1m.

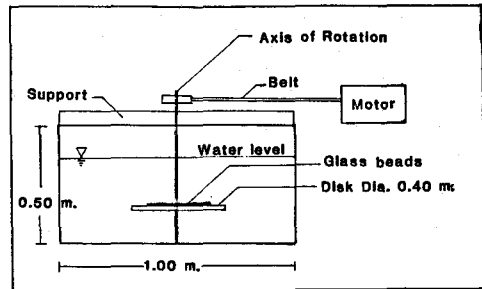


Fig.2 Experimental Apparatus

#### 5. Velocity Profiles

A wedge type hot-film probe was rotated along with the disk, so that the velocities very near to the disk could be measured. The rotating electric wires from the probe were immersed in two mercury containers, which in turn was connected to the anemometer. The

calibration was carried out in the same arrangement, but with the probe at a large distance from the disk, so that fluid at that position will not be affected by the motion of the disk for the first few seconds when the recording is carried out.

The fluid surface gradient was found to be negligible for the range of  $\omega$  considered. For the measurement of circumferential velocity the probe was attached to a gage which could be moved along a horizontal axis attached to the axle as shown in Fig.3. The velocity recorded with the pen-recorder is subtracted from the probe velocity to get the velocity of the fluid. The circumferential velocity could be measured up to the distance of 1mm from the disk. Boundary layer thickness was found to be greater than the particle size. A typical measured velocity profiles along with the Karman's velocity profile are plotted in non-dimensional form as shown in Fig.4. Unlike in Karman's case, the profiles are different at different radius  $r$ . It can be attributed to the presence of the axle and the finiteness of the disk and fluid.

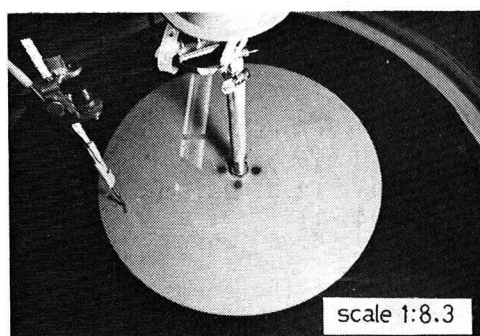


Fig.3 Experimental Set-up for Circumferential Velocity Measurement

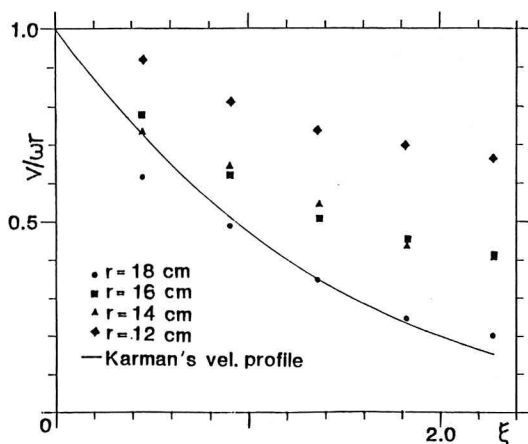


Fig.4 Circumferential Velocity Profile

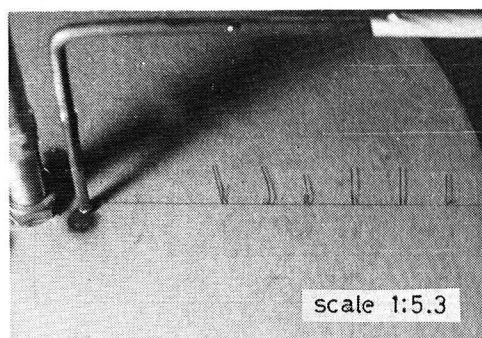


Fig.5 Experimental Set-up for measurement of angle  $\alpha$

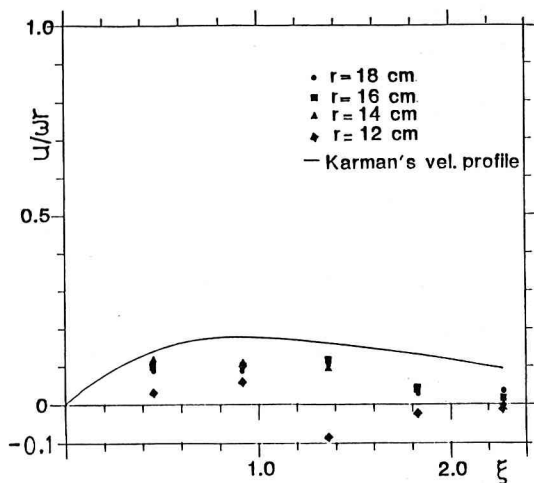


Fig.6 Radial Velocity Profile

Next, the angle  $\alpha$  between the resultant horizontal velocity and the circumferential velocity was measured by photographing the silk

tuft under the flow. The method utilized can be seen in the photograph shown as Fig.5. The radial velocity is then calculated as  $u=v\tan\alpha$ , and plotted in non-dimensional form as shown in Fig.6.

### 6.General description of the motion of particles

For the observation of the incipient motion of the particles, the stationary disk submerged in the fluid was first covered, as uniformly and completely as possible, with a single layer of glass beads. The disk is then slowly given a rotational speed. As the angular speed  $\omega$  of the disk increases, the particle beyond certain radius  $r$  starts to move outwards as shown in Fig.7. Unlike in the channels, there is no

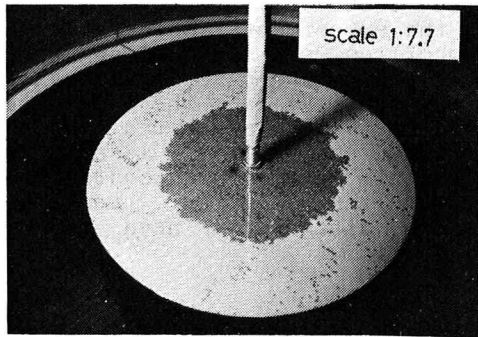


Fig.7 Motion of Particles on Rotating Disk

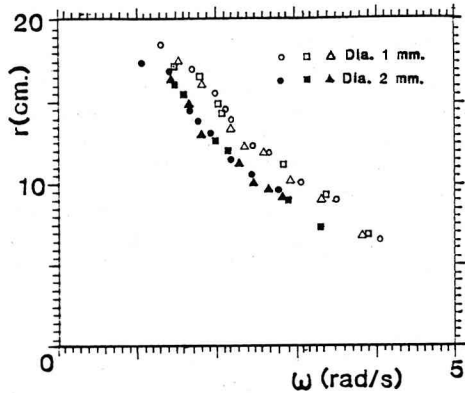


Fig.8  $\omega$ - $r$  relation for Initiation of Motion

difficulty involved in ascertaining the incipient motion of the particle here. Once the particle starts to move outwards, as the situation is more extreme outside, the particle gets accelerated and eventually falls out of the disk. At any angular speed  $\omega$ , once the particle beyond certain radius  $r$  moves out, that critical radius could be easily measured. As the disk was rotating, the radius could be measured by making two pointers, movable together on horizontal axis, collinear with the particle front. Various values of  $\omega$  and corresponding value of  $r$  are noted down. Three such runs were carried out for the particles of diameter 1mm and also repeated for diameter 2mm. The results are shown in Fig.8

### 7.Comparison between Experimental and Analytical results

The nondimensional velocities  $F(\xi)$  and  $G(\xi)$  and the velocity gradients  $F'(\xi)$  and  $G'(\xi)$  are found out from Figs. 4 and 6. Neglecting  $D_p$  and  $L_p$  as mentioned before, the critical tractive force equivalent was found analytically using Eq.2. The experimental and analytical results are compared in Fig.9. The results are fairly good for 2mm diameter particle but does not look promising for 1mm particle. It was found difficult to place one single layer of the particles on the disk, specially in the case of

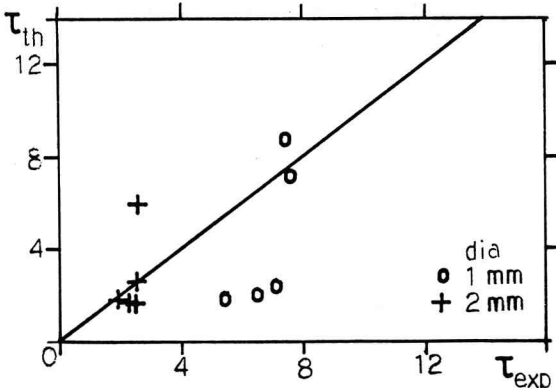


Fig.9 Comparison of Experimental and Analytical Critical Tractive Force Equivalent

1mm. particles. For the velocity measurement at each point, to position the probe the disk had to be stopped and rerotated at the same angular velocity. The sheltering effect, effect due to the depth of fluid, and any unevenness of the disk surface has not been taken into account. Moreover sufficient information is lacking regarding the lift force experienced by the particle under the type of flow field considered. Considering the experimental error involved in the many stages of observations, the results obtained can be said to be satisfactory.

#### 8. Concluding Remarks

An analytical expression for the critical tractive force equivalent was obtained and checked with the experimental observations. The circumferential and radial velocity profiles were measured and were found to be considerably different from that for the case of Karman's problem. The vertical component of the velocity and the pressure differences were not measured and their effects were neglected. Under such conditions, the critical tractive force equivalent could not be satisfactorily represented by the analytical expression considered. Further studies taking into account the sheltering effect, vertical velocity, surface roughness and pressure differences need to be conducted for the better representation.

#### References

- 1) Benton, E. R., "On the flow due to a rotating disk", J. Fluid Mech., vol. 24, part 4, pp. 781-800, 1966.
- 2) Cochran, W. G., "The flow due to a rotating disk", Proc. Camb. Phil. Soc., 30, pp. 365-375, 1934.
- 3) Englund, F., "The motion of sediment particles on an inclined bed", Prog. Rep. 53, Inst. Hydrodyn. and Hydraulic Engrg., Tech. Univ. Denmark, pp. 15-20, 1981.
- 4) Fair and Geyer, "Water supply and wastewater Disposal", John Wiley and Sons, Inc., N.Y., 1963.
- 5) Goldstein, S., "On the resistance to the rotation of disk immersed in a fluid", Proc. Cambr. Phil. Soc., 31, part 2, pp. 232-241, 1935.
- 6) Ikeda, S., "Incipient motion of sand particles on side slopes", Jour. of Hyd. Div., ASCE, vol. 108, No. HY1, pp. 95-114, 1982.
- 7) Iwagaki, Y., "Fundamental Study on Critical Tractive Force", Proc. JSCE, No. 41, pp. 1-21, 1956 (in Japanese).
- 8) McCormack, P.D., and Lawrence, C., "Physical Fluid Dynamics", Academic Press, Inc., N.Y., 1973.
- 9) Saffman, P.G., "The lift on a small sphere in a slow shear flow", J. Fluid Mech., vol. 22, part 2, pp. 385-400, 1965.
- 10) Schlichting, H., "Boundary Layer Theory", McGraw Hill Co., New York, 1968.